

## Supplementary Materials and Methods:

### Quantification of cMyBPC protein quantities in MYBPC3 variant mouse models

MyBPC was depleted in the hearts of mice by injection of MyBPC-RNAi at post-natal day 10 and by germline mutations in *Mybpc3* mutations that inserted the PKG-neomycin resistance gene insertion into one or both copies of exon 30. The resultant protein is truncated from 1270 amino acids to 1064 amino acids (Supplemental Figure 1A). Western blots of cardiac tissues demonstrate reduced cMyBPC quantities in the MyBPC-RNAi and *Mybpc3<sup>t/+</sup>* and *Mybpc3<sup>t/t</sup>* mice (Supplemental figure 1B). Densitometry of these blots indicated that cMyBPC protein quantities were  $\sim 35 \pm 8\%$  (*Mybpc3<sup>t/+</sup>*) and  $\sim 13 \pm 7\%$  (*Mybpc3<sup>t/t</sup>*) and absent in RNAi- treated mice (Supplemental Figure 1C).

### Western blot analysis of MyBPC phosphorylation in MyBPC t/+ and t/t mice.

Samples were homogenized in a urea lysis buffer (7M urea, 2M thiourea, 50mM tris-HCl (pH7.5), 0.4% CHAPS, 20mM spermine, 20mM DTT) containing protease and phosphatase inhibitors. Protein concentration was determined by Bradford assay, and 15ug used for SDS-PAGE. Gels were transferred for 3hrs at 300mA and blocked for 1 hour. Primary antibodies were used as follows: pSer282 - 1:2,000; pSer302 - 1:10,000 (all rabbit); Total cMyBP-C (Santa Cruz E7, 1:2,000 mouse). Beta actin (Prosci - 1:5,000 rabbit) was used as a loading control. Primary antibodies were detected with Licor IRDye goat anti-rabbit 800CW or goat anti-mouse 680RD ( both 1:10,000). n=4 for WT, 3 for t/+ and t/t.

### In vivo comparisons of *Mybpc3* mouse models

Echocardiography of *Mybpc3<sup>t/+</sup>* and MyBPC-RNAi mice (Supplemental Figure 2A) showed comparable fractional shortening (FS) to wildtype (WT) and sham-injected mice across study ages (5-20 weeks). By contrast fractional shortening of the DCM model, *Myh6<sup>F764L/F764L</sup>* is reduced<sup>34, 35</sup>. MyBPC-RNAi caused mild increased left ventricular posterior wall (LVPW) thickness compared to WT and *Mybpc3<sup>t/+</sup>* mice at 20 weeks (Supplemental Table 1 and Figure 2B). MyBPC-RNAi reduced cMyBPC RNA quantities < 10% of sham control (Supplemental Figure 2C).

### Characterization of viral titers for *Mybpc3* expression depletion

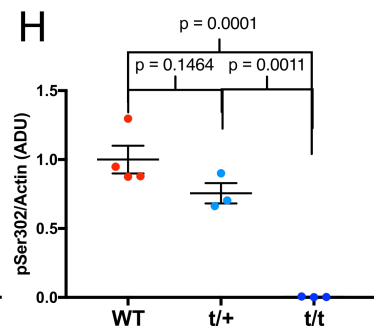
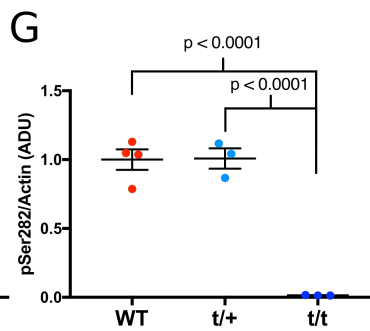
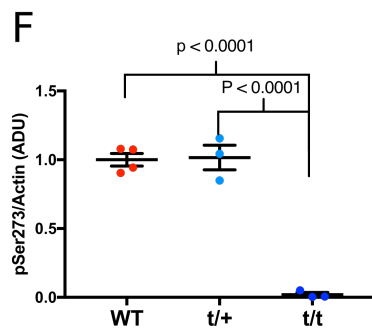
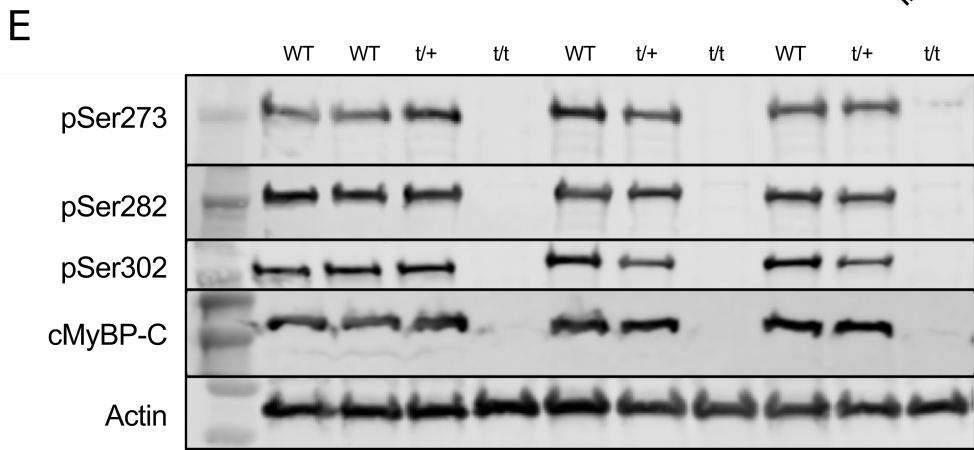
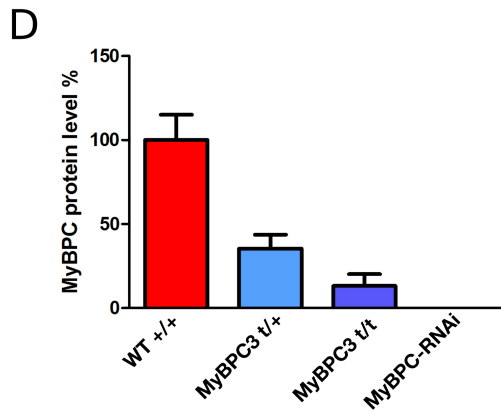
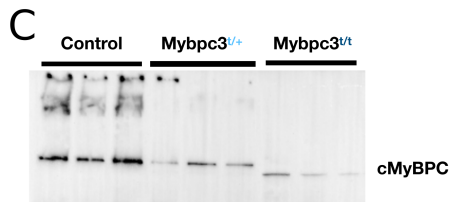
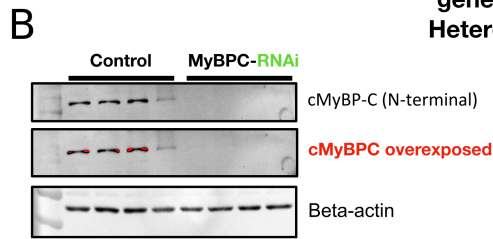
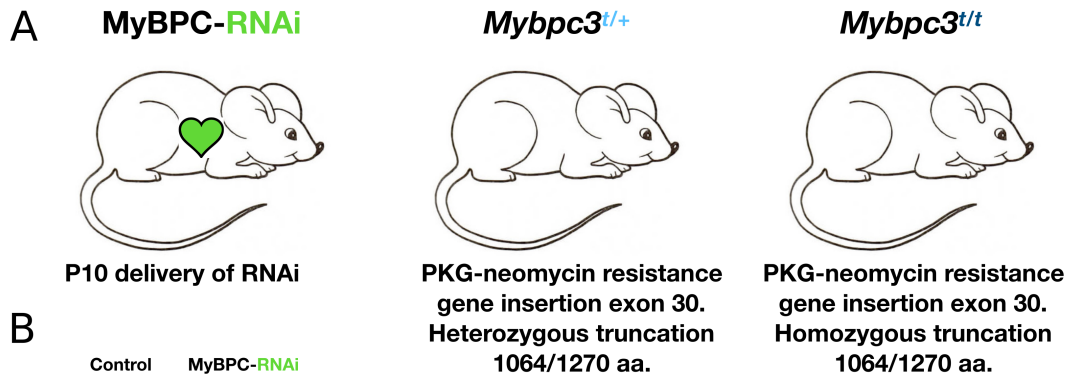
Assessments of *Mybpc3* expression were performed and normalized to beta actin in response to increasing viral titers of MyBPC-RNAi virus (Supplemental Figure 4A). *In vivo* measurement of left ventricular posterior wall (LVPW) dimensions correlated with increasing viral titer (Supplemental Figure 4B).

### Assessing fluorescent decay in Mant-ATP experiments

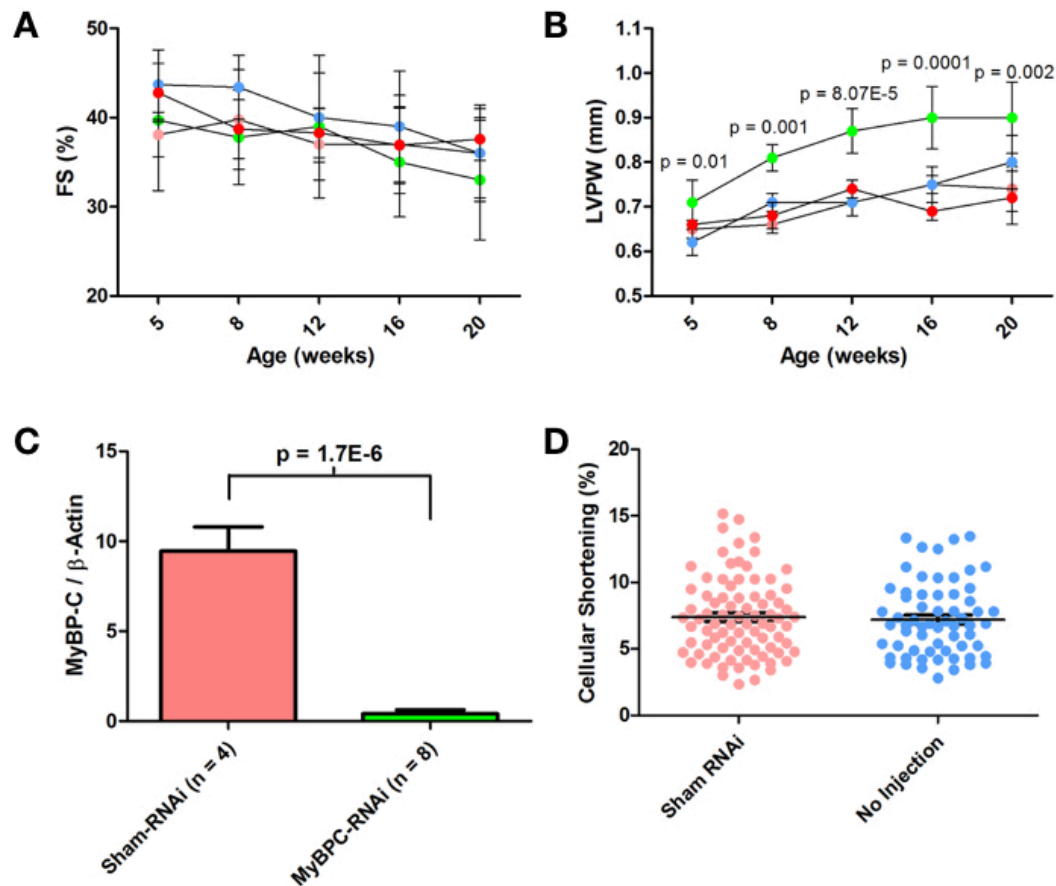
By measuring fluorescent intensity decay over multiple sections of chemically permeabilized myocardium we assessed the ratio between the amplitudes of the fast and slow decays of a double exponential fluorescent decay (Supplemental Figure 5A). We provide a movie of this decay in a section of skinned myocardium that has been imaged as indicated in the methods section (Supplemental Figure 5B)

### Mant-ATP assay measures of myosin DCM on SRX/DRX ratios in *Mybpc3<sup>t/t</sup>* mice

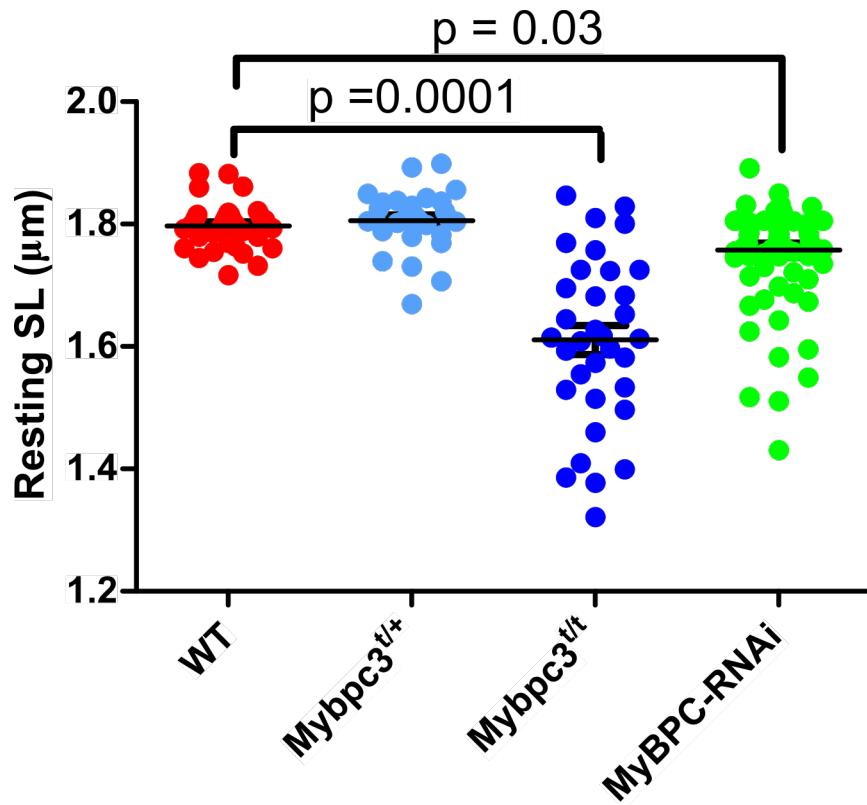
Mant-ATP assays performed on permeabilized myocardium Myh6<sup>764/764</sup>, Myh6<sup>764/764</sup>x Mybpc3<sup>+/+</sup> and Mybpc3<sup>+/+</sup> mice. Myh6<sup>764/764</sup> showed no statistically significant change (p = 0.053) in SRX and DRX ratios (Supplemental Figure 6).



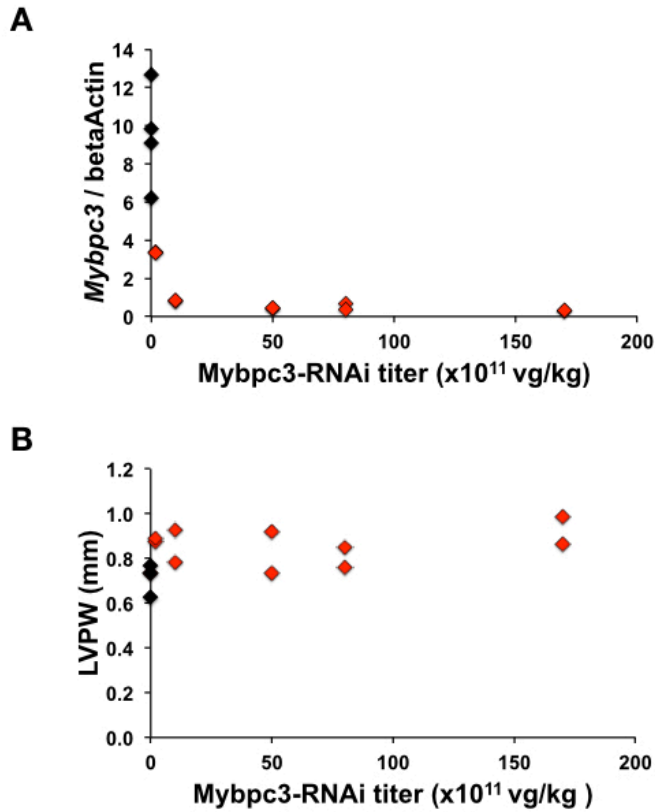
**Supplemental figure 1: *Mybpc3* mouse models.** **A)** Pictorial representation and description of murine models used to assess cMyBPC deficiency on cellular function. **B-C)** Western blots of cMyBPC extracted from the myocardium of MyBPC-RNAi<sup>51</sup> and from *Mybpc*<sup>t/+</sup> and *Mybpc*<sup>t/t</sup> mice demonstrates reduces cMyBPC protein expression. **D)** Densitometry of blots quantifies the reduction of cMyBPC in each genotype. **E)** Representative blots indicating phosphorylation site and genotype. **F-G)** Normalized phosphorylation of WT, t/+ and t/t mice, significances shown on each graph indicate differences between t/t and t/+ or WT genotypes. N corresponds to the amount of animals sampled shown as discrete dot on the plot.



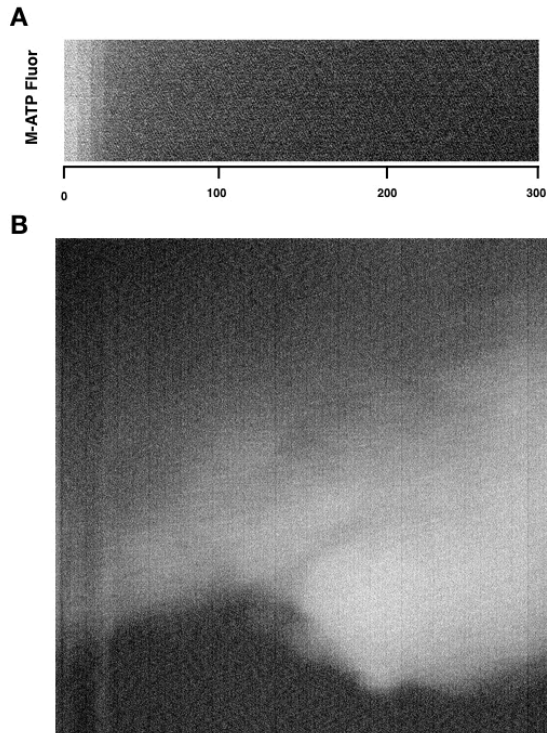
**Supplemental Figure 2: *In vivo* cardiac function and proteomic characterization in MyBPC models.** **A)** Fractional shortening of mouse genotypes including MyBPC-RNAi (Green, n=8), Mybp3<sup>+/+</sup> (Blue, n=4), Sham-RNAi of Mybp3<sup>+/+</sup> (Pink, n=4), and WT (Red, n=4), as a function of age (weeks). Note that pink and red symbols overlap. **B)** Left ventricular posterior wall (LVPW) dimensions of mice as a function of age (weeks). **C)** Quantities of cardiac tissue *Mybp3* RNA in comparison to  $\beta$ -actin in Sham-RNAi and MyBPC-RNAi mice. **D)** Cellular shortening, a measure of contractility in Sham-RNAi (no Mybp3-RNAi) and Mybp3<sup>+/+</sup> mice shows no effect of vector injection on contractility.



**Supplemental Figure 3: Resting SLs of animal models studied.** Plot showing the data dispersion and mean of resting SLs in un-loaded mouse myocytes. All significances are indicated in relation to WT with a significance cut off of  $p < 0.05$ .

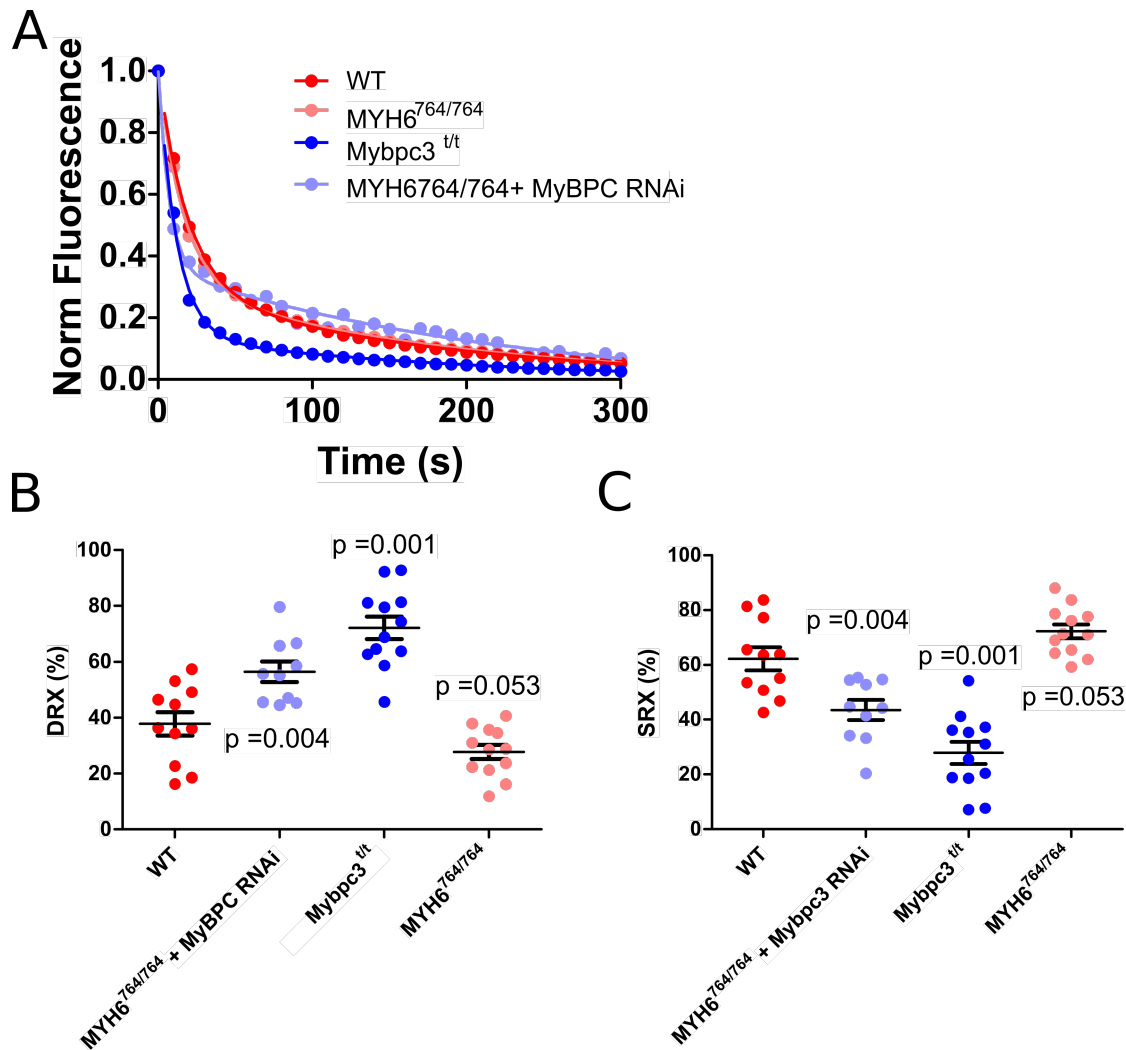


**Supplemental Figure 4: The protein and function effects of increasing Mybpc-3-RNAi titers. A)** *Mybpc3* transcripts, normalized for beta actin expression, in mice treated with increasing titers of Mybpc-3-RNAi (red diamonds) and untreated mice (black diamonds). **B)** Viral titer correlated with left ventricular posterior wall (LVPW) dimensions in mice treated with Mybpc-3-RNAi (red diamonds) compared to untreated mice (black diamonds).



**Supplemental Figure 5: Analysis of Mant-ATP video files.** **A)** Representative fluorescence change per frame imaged throughout a Mant-ATP dark ATP chase, frame capture is every 10 seconds. **B)** Frame from a representative movie showing a section of myocardium during fluorescent washout, frame capture rate is once per 10 seconds and decays were imaged for 15 minutes. See Movie S1 for fluorescence washout.





**Supplemental Figure 6: Mant-ATP assays in cardiac tissues for Myh6<sup>764/764</sup> mice with DCM nad Myh6<sup>764/764</sup> + Mybpc3 RNAi.** **A)** Average Mant-ATP fluorescence decay curves of myocardium from Myh6<sup>764/764</sup>, Myh6<sup>764/764</sup> x MyBPC RNAi and Mybpc3<sup>t/t</sup> mice (n= 3 for each genotype, with 4 experiments per mouse). Data is fit by double exponential decay to assess ratios of DRX and SRX heads in the myocardium. **B)** Plot of the initial rapid decay amplitude corresponding to DRX heads. Data are plotted with mean ± SEM indicated. **C)** Plot of the second exponents of slow decay amplitude corresponding to SRX heads. Data are plot with mean ± SEM indicated. All significances are indicated with corresponding p values in relation to WT.

**Supplemental Movie S1: The fluorescent decay during dark ATP chase of Mant-ATP in permeabilized myocardium.** A single frame is provided in Supplemental figure 5B.

	WT 5 weeks		WT 20 Weeks		MyBPC <sup>t/+</sup> 5 weeks		MyBPC <sup>t/+</sup> 20 weeks		MyBPC-RNAi 5 weeks		MyBPC-RNAi 20 weeks	
	Naive	+461	Naive	+461	Naive	+461	Naive	+461	Naive	+461	Naive	+461
<b>LVPW (mm)</b>	0.66± 0.02	0.66± 0.01	0.72± 0.03	0.72± 0.06	0.65± 0.02	0.72± 0.01*	0.74± 0.05	0.78± 0.06	0.70± 0.03	0.76± 0.04	0.95± 0.05	1.0± 0.03
<b>FS (%)</b>	43±1.6	40 ±1.3	37±1.2	30 ±2.6*	39.8±5.6	40±1.6	36±2.7	27±4.5*	42±3.9	37±2.9	36±2.9	31±1.6*

**Supplemental Table 1:** Echocardiographic parameters of WT, MyBPC<sup>t/+</sup>, and MyBPC-RNAi at baseline and after MYK-461 treatment for 5 and 20 weeks. Additionally MyBPC<sup>tt</sup> LVPW at baseline was measured as 1.0 ± 0.03 at 5 weeks and 1.0 ± 0.05 at 20 weeks. MyBPC<sup>tt</sup> FS was also assessed at baseline at 5 weeks 26 ± 2.4 and 20 weeks 24 ± 2.4. \*denotes statistical significance (p < 0.05) between MYK-461 naive and treated within each genotype. MYK-461 was administered at 2.5 mg/kg per day via drinking water.